



Modification of Paschen's Law for Electrodes with Different Shapes and Materials Using DC Nitrogen Glow Discharge

S. I. Radwan^{1*}, Ahmed Azouz², S. M. Abdel Samad³ and H. El-Khabeary¹

¹Accelerators and Ion Sources Department, Nuclear Research Center, Egyptian Atomic Energy Authority, Egypt

²Avionics Department, Electrical Engineering Branch, Military Technical College, Kobry El-Kobba, Egypt

³Experimental Nuclear Physics Department, Nuclear Research Center, Egyptian Atomic Energy Authority, Egypt

In this manuscript, d.c. glow discharge of conical, hemispherical, and spherical electrodes made of different materials was measured using nitrogen gas. The electrodes' materials from aluminum, graphite, and stainless steel were used. From the experimental results, the work function of anode and cathode materials with different shapes play an important role in the electrical discharge characteristics and Paschen curves. It was found that the cathode material with a low work function and large surface area became a control factor in the determination of the low breakdown voltage ($V_{b\text{minimum}}$) values. In addition, the work function of different materials for conical anode or conical cathode with hemispherical and spherical cathode or anode had the minimum values of breakdown voltages. In Paschen curves, the hemispherical anode and cathode with the same and different materials gave a small difference in their values. The conical stainless steel cathode gave the lowest values of Paschen curve in a comparison between different materials of conical cathodes in cases of hemispherical aluminum anode and spherical graphite one. In addition, the conical graphite anode gave the lowest values of Paschen curve in case of the hemispherical aluminum cathodes. The modified Paschen's law indicated that the breakdown voltage was not only as a function in the product of gas pressure and inter-electrode distance but also the ratio of materials' work functions and surface areas of electrodes. It was deduced in a general formalism according to the materials and shapes of cathodes for discharge cases having the same ($V_{b\text{min}}$) value.

Keywords: Paschen's law, Minimum breakdown voltage, Gas discharge, Glow electrical discharge.

1. Introduction

In electrical discharge of gases, the ionized gas was consisted of the neutral, negatively and positively charged particles. Irving Langmuir defined the plasma term as the fourth state of matter which resulted from wholly or partially ionization of gas. He discovered the plasma oscillations in the ionized gas [1]. Gas discharge plasma consists of neutral particles, electrons, ions, photons, metastable particles and radicals with the same density of electrons and ions [2, 3]. When a high voltage is applied between two parallel plate electrodes (anode and cathode) in a chamber at a low gas pressure, the molecules of gas will be changed from their gas state to the plasma one [4]. The breakdown voltage occurred when the voltage raised to a certain degree at which the gas converted to glow or spark discharge. Also, it indicates the transition from a non-self-sustaining discharge to a self-sustaining one. Hence, the plasma was generated and then known as the d.c. glow discharge or cold plasma. In this discharge, the electric field was homogeneous and the secondary electrons were created due to the strike of ions with the cathode. Then the avalanche of electron generates more electrons than ions as the electrons are faster than ions. These electrons are drifted and quickly directed into the anode and then absorbed. After that, the ions are owing a lot of inertness and piling up in the gap between electrodes. So, the number of ions are accumulated and grown until reached a threshold accumulation. Therefore, the electric field is not yet homogeneous and decreases on the side of anode. This leads to the slowing down of the electrons which move towards the anode. This process continues until the electric field disappears at the anode. Then, the electrons can't yet go over freely to the anode and are frequently gone slowly. The number of electron density increases until the ions' density decreases, and subsequently, plasma is composed close to the anode. The plasma expands from the anode to cathode due to the increase in the number of charged particles. So that the

*Corresponding author: *e-mail: samahtorab1983@gmail.com

DOI: 10.21608/EJPHYSICS.2023.189836.1086

Received: 26/1/2023; Accepted: 22/2/2023

©2023 National Information and Documentaion Center (NIDOC)

plasma extension compresses the region of strong field towards the cathode. These phenomena go ahead until the generation of charged particles is equilibrated, i.e., the generation and losses are equal. So, the two regions of the sheath and plasma will be appeared.

The voltage required to start the electrical discharge through the gas and exceeds a certain value, known as the breakdown voltage (V_b), [5]. Müller and De La Rue observed that the breakdown voltage depends on the product of gas pressure and the inter-electrode distance between the two planar electrodes [6]. F. Paschen sophisticated a law which states that the electrical breakdown voltage as a function in the product of working pressure (P) and the gap distance between electrodes (d). This law is known as the Paschen's law and expressed as [7]:

$$V_b = f(Pd) \quad (1)$$

A Paschen curve is plotted by making Pd along the x-axis and V_b along the y-axis [8-10]. Paschen discovered that the application of d.c. voltage between two parallel plate electrodes and formed the homogeneous field. When the numerical value of Pd is changed, the breakdown voltage has a minimum value, $(V_b)_{min}$. The validity of Paschen's law is confirmed for various d.c. discharge conditions such as distances, pressures, and electrode materials [11, 12]. The departures from Paschen's law have been observed at small electrode gaps [13, 14].

Various technologies are depending on the electrical gas discharge such as the ion sources, accelerators, plasma sterilization, thin film deposition, atmospheric pressure, plasma jets, etc. [12, 15-23]. Applications of d.c. glow discharge at the ambient and low pressures are including the surface cleaning, microelectronic industry, surface modification, thin films surface deposition for electrical devices, plasma polymerization, biomaterials' applications, etc. [24-29].

Various literatures presented that the conventional Paschen's law is verified for two parallel plate electrodes [30-34]. On the contrary, some experiments proved that this law does not verify for the gas discharge tubes with $d/r \gg 1$, where d: the inter-electrodes distance and r: the electrode radius [5, 35-39]. This leads to the modification in Paschen's law in which the gas breakdown voltage as a function of Pd value and the ratio of the gap distance to the electrode radius [$V_b = f(Pd, d/r)$] for large discharge gaps [5]. In a uniform d.c. electric field, the gas breakdown was studied for several materials of cathode, gap distances, and radii of discharge tube [40-42]. So the Paschen's law was modified in which the breakdown voltage as a function of both Pd and d/R, where R is the radius of discharge tube. For $d/R \leq 1$, Paschen's law can be applied for a short discharge tube. For $d/R > 1$, the breakdown curve moves towards lower pressure values and higher V_b when the gap distance increases [42]. Furthermore, the experiments proved that the Paschen curves for several gas discharge tubes are overlapped if the d/r value is kept constant [43]. Because the first ionization coefficient and mean free path of electrons are an exponential function of the electric field and they result in the intersection.

In this work, the electrical electrodes with different shapes and materials was used because it has an important role in the characteristics of discharge devices such as:

a- Removal of air pollutants

Air pollutants such as nitrogen oxides (NO_x), unburned hydrocarbons, carbon monoxide were released into the atmosphere by various sources. These sources are the burning of electric generating plants using coal, oil and natural gas, paper mills, diesel engine exhausts, motor vehicles, etc. [44]. A dry NO_x removal technology is one of the candidates to solve this problem in the traditional processes. An attractive process for this technology is a dielectric barrier discharge DBD which is a non-thermal plasma process. Because it can be operated with a stable way at atmospheric pressure by the ozone generator [45]. Where, the diesel engine exhaust gas was carried out using a DBD for various geometries of the electrode to enhance the removal efficiency.

b- Gas switches

The gas switches can be used in the systems of high voltage pulsed power due to their high voltage and power. In these systems, the estimation of breakdown voltage of high pressure in gas switches was based on Paschen's law. Among the vacuum switches, the thyatrons operated on the left side of the Paschen curve. While the pressurized spark gaps worked on the right side [46]. Otherwise, the micro-electromechanical systems were usually concerned with the middle region of Paschen curve. The minimum point in Paschen curve is important in the design of systems that will never subject to the breakdown voltage with any gap distance for a given pressure. As long as, it is operated below the

maximum threshold voltage. The Pd regime and the lowest point in Paschen curve is essential for various practical applications [47-49]. The breakdown voltage is strongly dependent on the cathode material, surface roughness, and whether the generated breakdown in dc or rf mode [50, 51, 12].

c- Ionization gas sensors

The performance of any gas sensor is verified by the Paschen curve [52]. The ionization gas sensors are essential in the nuclear power plants in order to detect the toxic gases for the safety of facility. Also, they are used in the space missions where the operation of low power and compactness are necessary.

d- Plasma jets

In physics of plasma jets, the influence of different components of jet systems on the dynamics of discharge such as the electrodes, target, tube, etc. [53, 54].

e- Electron guns

The electrodes' geometry effected on the performance of electron gun [55]. Where the main beam optics are consisting of beam waist, uniform flow of electrons, defocusing and focusing, and the axial location of beam spot [56]. The high current electron sources are used for electron accelerator, welding of metals, ion cooling system, etc.

Experimental Setup

D.C. glow electrical discharge was studied between the two electrodes, anode (A) and cathode (K), with the same / different shapes and materials. The hemispherical, conical and spherical shapes made of different materials as graphite, C, aluminum, Al, and stainless steel, SS, were investigated. The different discharge cases under study were presented in the following Table (1):

TABLE 1. D.C. Glow electrical discharge cases for anode and cathode electrodes with same / different shapes and materials

Sub-case	A		K	
	Shape	Material	Shape	Material
1	Hemisphere	Al	Hemisphere	Al
2	Hemisphere	Al	Hemisphere	C
3	Hemisphere	C	Hemisphere	Al
4	Hemisphere	Al	Conical	Al
5	Hemisphere	Al	Conical	C
6	Hemisphere	Al	Conical	SS
7	Conical	Al	Hemisphere	Al
8	Conical	C	Hemisphere	Al
9	Conical	SS	Hemisphere	Al
10	Sphere	C	Conical	C
11	Sphere	C	Conical	SS
12	Conical	C	Sphere	C
13	Conical	SS	Sphere	C
14	Conical	Al	Conical	Al
15	Sphere	Al	Sphere	Al

Figure (1) shows the electrical circuit of d.c. glow electrical discharge between the hemispherical (Al) anode and cathode using nitrogen (N_2) gas. The electrodes were fixed on two Teflon insulator flanges at the ends of the cylindrical electrical discharge tube. The inter-distance between the electrodes was fixed at 9 cm. Teflon flanges of 15 cm outer diameter and 1.2 cm thickness was used. A Pyrex glass electrical discharge tube of 23 cm length, 10 cm inner diameter and 0.3 cm thickness was used. An Edwards rotary pump was connected with the electrical discharge tube from one side to evacuate until 10^{-3} Torr. The pressure inside this tube was measured using a digital vacuum meter (Pfeiffer vacuum meter D-35614 Asslar). On the other side of tube, the nitrogen gas of 99.99 % purity was admitted using a high sensitive needle valve to control and regulate its flow rate.

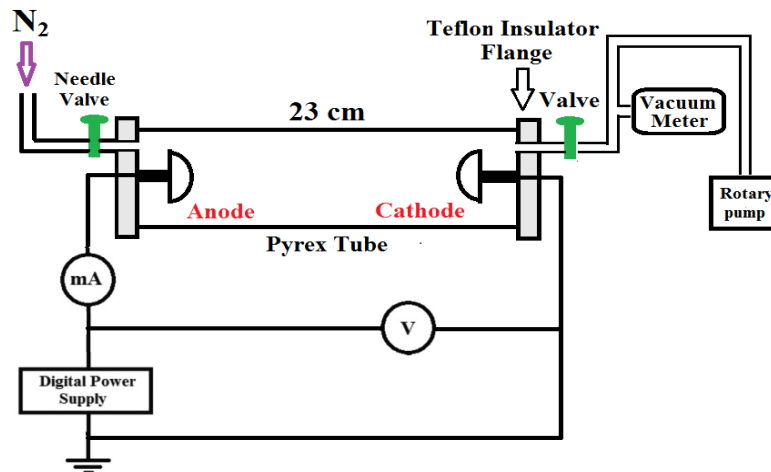


Fig. 1. D.C. glow electrical discharge circuit between hemispherical anode and cathode using N_2 gas.

The novelty of this work was focused in the following points:

- 1- Study the electrical discharge characteristics between the two electrodes, anode and cathode, at a constant gap distance with the same / different shapes and materials.
- 2- Investigate the Paschen curves for these discharge cases.
- 3- Modify the Paschen's law as a function of the materials and shapes of electrodes.
- 4- Deduce the general formula of Paschen's law according to the different materials and shapes of cathodes.

Results and Discussions

(A) Electrical discharge characteristics for electrodes with different shapes and materials

In this part, the breakdown voltage was plotted versus the electrical discharge current for the different materials, shapes, and polarity of electrodes.

1- Materials of electrodes

In this section, the breakdown voltage versus electrical discharge current curves for (Al and C) hemispherical electrodes and compared with (Al) hemispherical ones. Figure (2) illustrated the flowchart for the different cases of electrical discharge which was studied to modify Paschen's law.

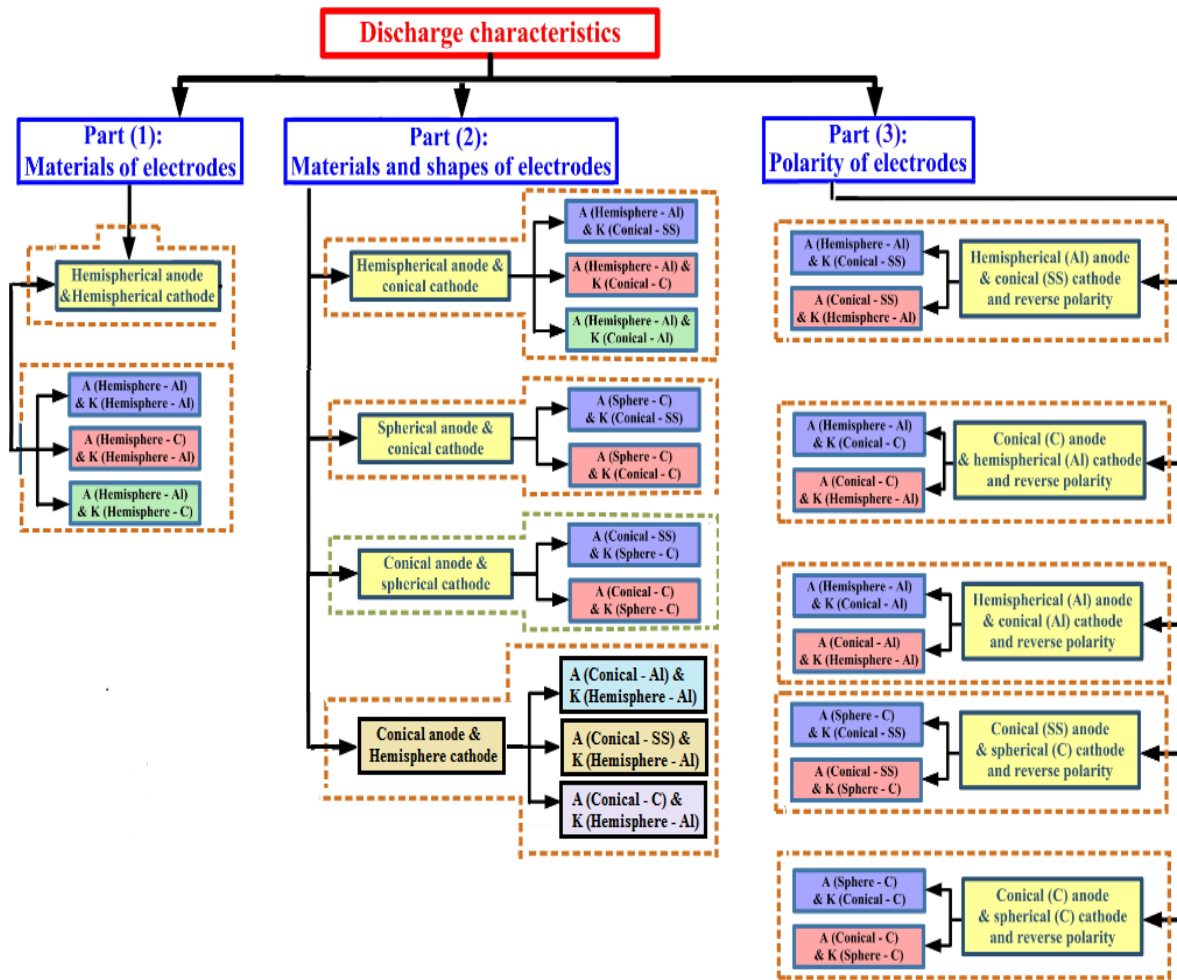


Fig. 2. Flowchart of different cases for d.c. glow electrical discharge using nitrogen gas.

1.1- Hemispherical anode and cathode

Figure 3 illustrated the relation between the breakdown voltage and electrical discharge current for:

- i- A: Hemispherical (Al) - K: Hemispherical (Al)
- ii- A: Hemispherical (C) - K: Hemispherical (Al)
- iii- A: Hemispherical (Al) - K: Hemispherical (C)

This Figure includes a Table that represents the goodness of fit and root mean square (RMS) error of values, and standard deviation (SD). In addition to the minimum breakdown voltage (V_b)_{min}, and electrical discharge current (I_d) at this minimum voltage for each case. The hemispherical (Al) anode and cathode was the highest goodness of fit and the lowest RMS error, SD and I_d . The hemispherical (Al) anode with hemispherical (C) cathode had the highest values of electrical discharge current. The cathode in the two cases of low work function material ($\phi_{Al} = 4.28$ eV) gave the low values of electrical discharge current than (C) one. Because the secondary electron emission coefficient depends on the surface nature and impurities which may increase the emission coefficient. So the (C) cathode gives the highest electrical discharge current. The hemispherical (Al) anode and cathode had the lowest values of electrical discharge current. This was due to the low work function material, Al, had the high secondary electron emission. Then the mean free path of electron decreased and as a result the ionization decreased and the recombination increased.

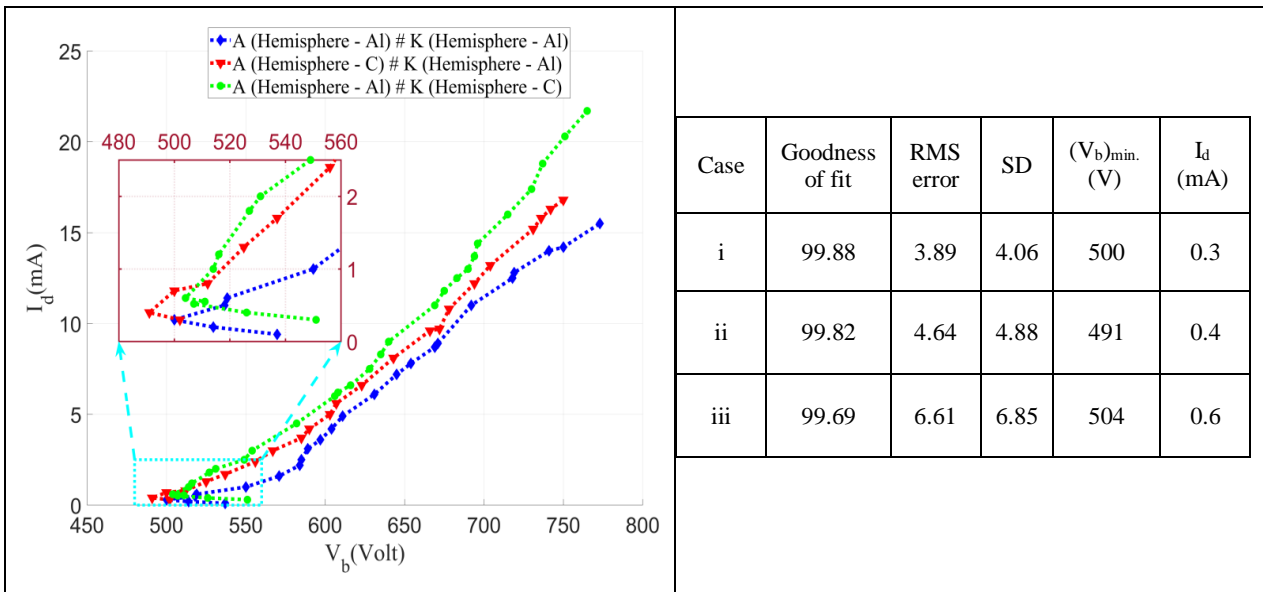


Fig. 3. Breakdown voltage versus electrical discharge current for the hemispherical (Al, C) anodes with hemispherical (C, Al) cathodes and compared with hemispherical (Al) electrodes.

2- Materials and shapes of electrodes

2.1- Hemispherical anode and conical cathode

Figure 4 illustrated the relation between the breakdown voltage and electrical discharge current for:

i- A: Hemispherical (Al) - K: Conical (Al)

v- A: Hemispherical (Al) - K: Hemispherical (Al)

ii- A: Hemispherical (Al) - K: Conical (C)

iv- A: Conical (Al) - K: Conical (Al)

iii- A: Hemispherical (Al) - K: Conical (SS)

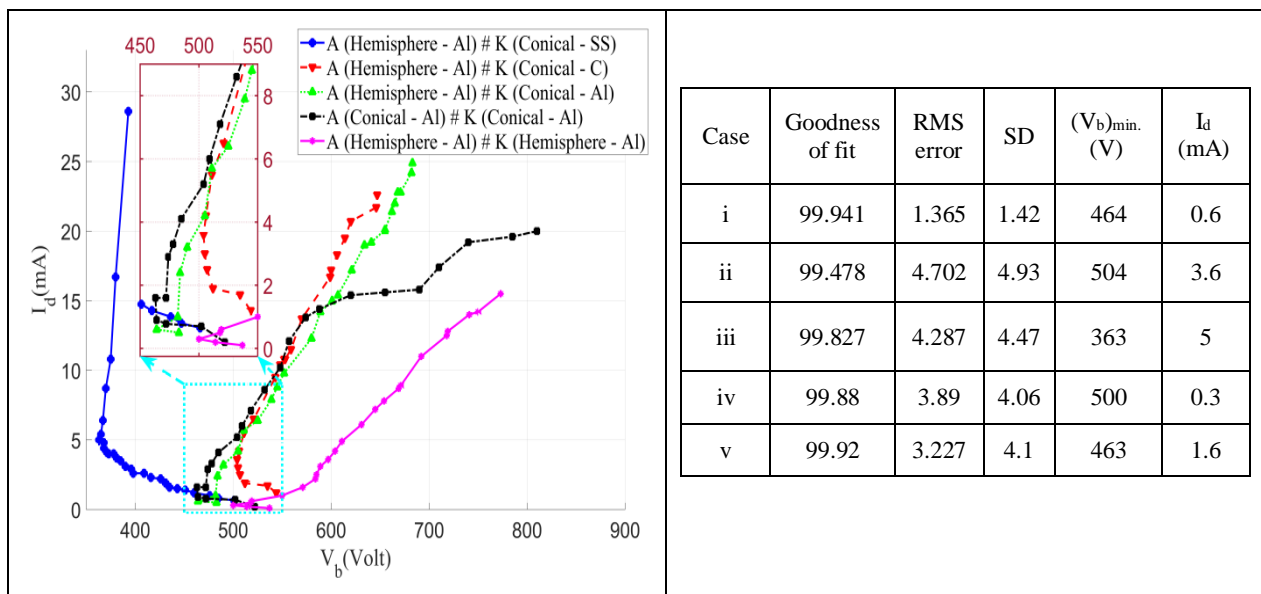


Fig. 4. Breakdown voltage versus electrical discharge current for hemispherical (Al) anode with conical (SS, C, Al) cathodes and compared with conical and hemispherical (Al) electrodes.

The hemispherical (Al) anode with conical (Al) cathode had the highest goodness of fit, and the lowest values of RMS error and SD. The hemispherical (Al) anode with conical (SS) cathode had the lowest value of $(V_b)_{min.}$. It had the highest values of electrical discharge current, while the hemispherical (Al) anode and cathode had the lowest ones. This means that the cathodes of same shape and low work function material gave the lowest value of electrical discharge current as discussed in Figure (3). The

cathode of work function material (SS) gave the highest electrical discharge current because of the recombination decreased due to its surface nature.

2.2- Spherical anode and conical cathode

Figure 5 illustrated the relation between the breakdown voltage and electrical discharge current for:

- i- A: Spherical (C) - K: Conical (C)
- ii- A: Spherical (C) - K: Conical (SS)
- iii- A: Conical (Al) - K: Conical (Al)
- iv- A: Spherical (Al) - K: Spherical (Al)

The spherical (C) anode with conical (C) cathode had the highest values of goodness of fit than spherical (C) anode with conical (SS) cathode. The conical (SS) cathode had the lowest values of RMS error, SD, $(V_b)_{min}$, and I_d than conical (C) one. The spherical (C) anode with conical (SS) cathode had the highest values of discharge current and the spherical (Al) anode and cathode gave the lowest ones. In the spherical anode and cathode, the secondary electron emission increased as the low work function materials of electrodes. So the ionization was decreased due to the small mean free path of electrons due to the small surface area of cathode. In conical cathode shape, the charges were concentrated at the tip of cone. Moreover, the conical (SS) cathode had the highest discharge current than the conical (C) one. Due to the low recombination and hence the great ionization efficiency which was appeared in case of the stainless steel cathode.

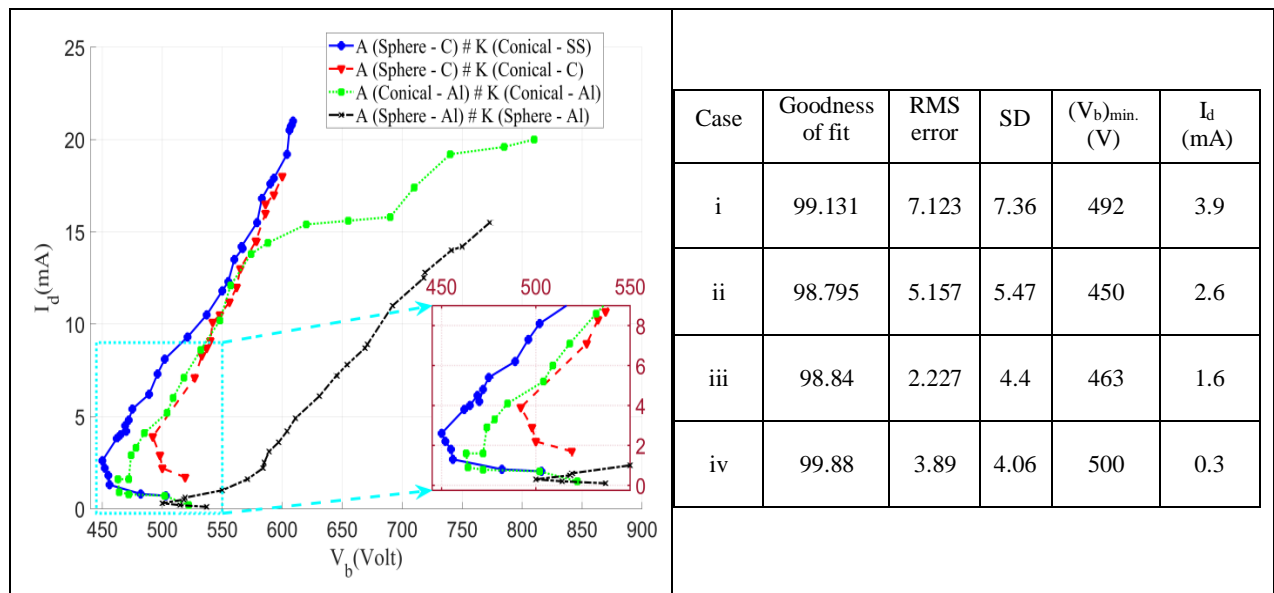


Fig. 5. Breakdown voltage versus electrical discharge current for spherical (C) anode with conical (SS, C) cathodes and compared with conical and hemispherical (Al) electrodes.

2.3- Conical anode and spherical cathode

Figure 6 illustrated the relation between the breakdown voltage and electrical discharge current for:

- i- A: Conical (C) - K: Spherical (C)
- ii- A: Conical (SS) - K: Spherical (C)
- iii- A: Spherical (C) - K: Conical (C)
- iv- A: Spherical (C) - K: Conical (SS)

The conical (C) anode with spherical (C) cathode had higher value of goodness of fit and lower values of RMS error, SD and I_d than the conical (SS) anode with spherical (C) cathode. The spherical (C) anode with conical (SS) cathode had the highest values of electrical discharge current and the conical (C) anode with spherical (C) cathode gave the lowest values. It was noticed that the cathode of low work function material (SS) with large surface area of cone (43.88 cm^2) had the highest electrical discharge current. In addition, the cathode of high work function material (C) with small surface area of sphere (5 cm^2) had the lowest values. This was due to the higher concentration of charges at conical (SS) cathode than that of spherical (C) cathode as discussed in Figure (5). Moreover, the cathodes of large surface areas with low or high work function materials gave the highest electrical discharge current.

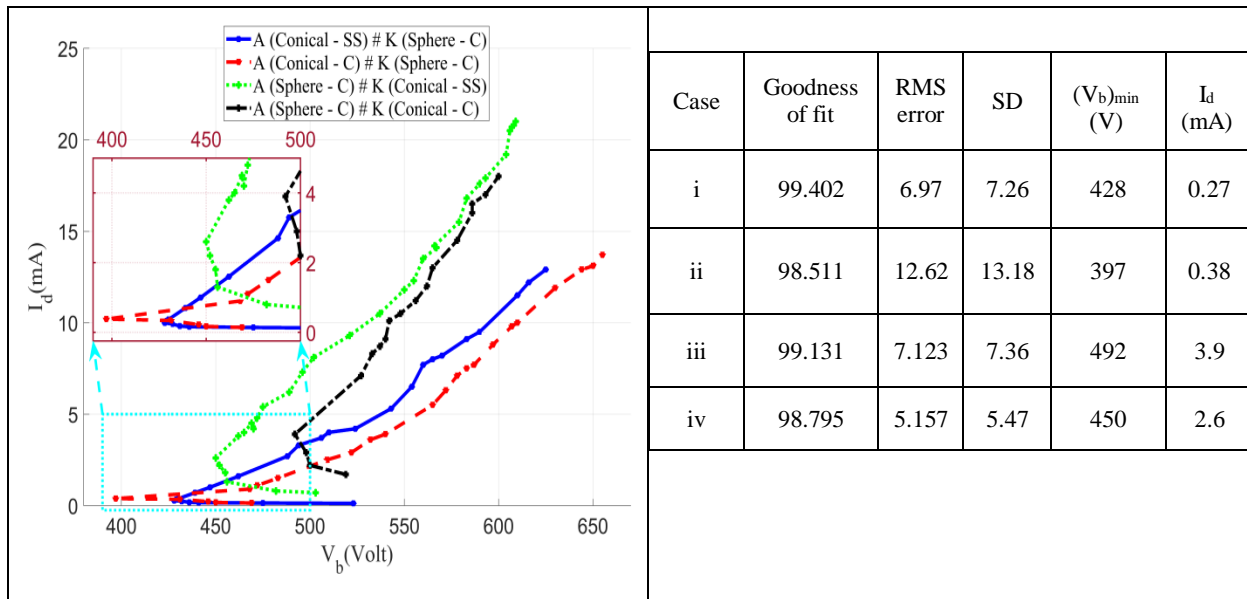


Fig. 6. Breakdown voltage versus electrical discharge current for (SS, C) conical anodes with (C) spherical cathode and compared with the reverse polarity.

2.4- Conical anode and hemispherical cathode

Figure 7 illustrated the relation between the breakdown voltage and electrical discharge current for:

- i-A: Conical (Al) - K: Hemispherical (Al)
- ii- A: Conical (C) - K: Hemispherical (Al)
- iii- A: Conical (SS) - K: Hemispherical (Al)

The conical (Al) anode with hemispherical (Al) cathode had the highest values of goodness of fit and the lowest values of RMS error and SD. The conical (C) and (Al) anodes had the highest and lowest values of the discharge current, respectively. Because the highest number of secondary ions which emitted from the material of anode with low work function (Al).

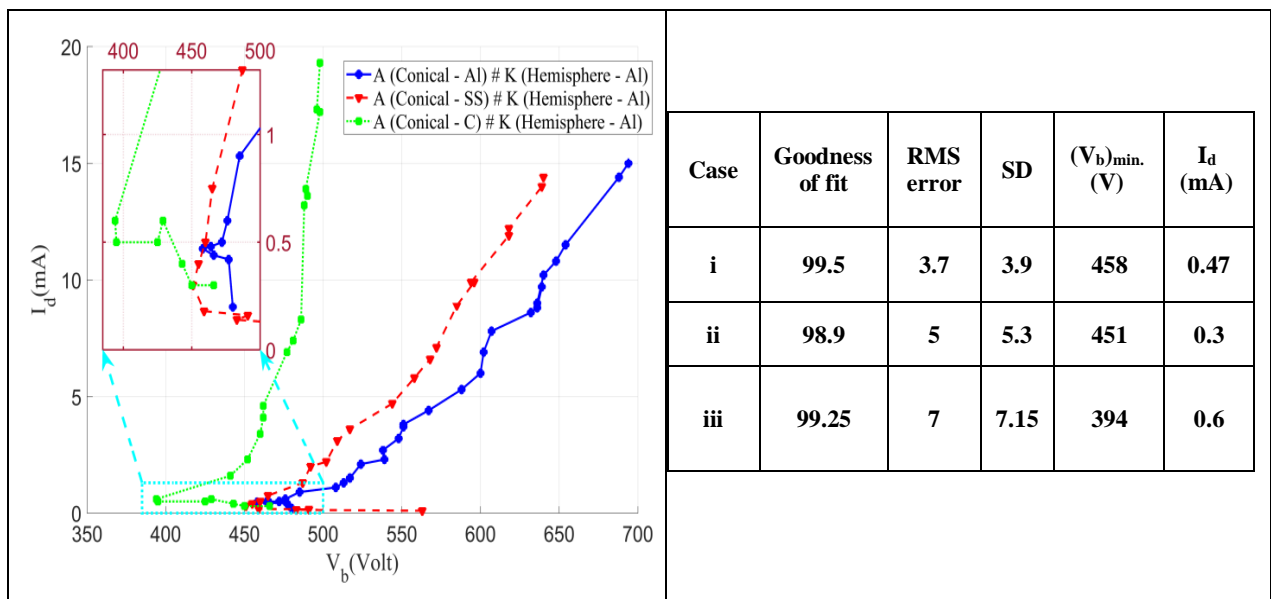


Fig. 7. Breakdown voltage versus electrical discharge current for (Al, SS, C) conical anodes and (Al) hemispherical cathode.

3- Polarity of electrodes

3.1- Hemispherical (Al) and conical (SS) electrodes

Figure 8 illustrated the relation between the breakdown voltage and electrical discharge current for:

i- A: Hemispherical (Al) - K: Conical (SS)

ii- A: Conical (SS) - K: Hemispherical (Al)

The hemispherical (Al) anode with conical (SS) cathode had the highest values of electrical discharge current. Because the conical (SS) cathode has a tip which allowed the charges to be concentrated and the electrical discharge current is increased. Moreover, the conical (SS) cathode had the lower $(V_b)_{min}$ value than hemispherical (Al) one. Because of the large surface area of conical cathode than hemispherical one.

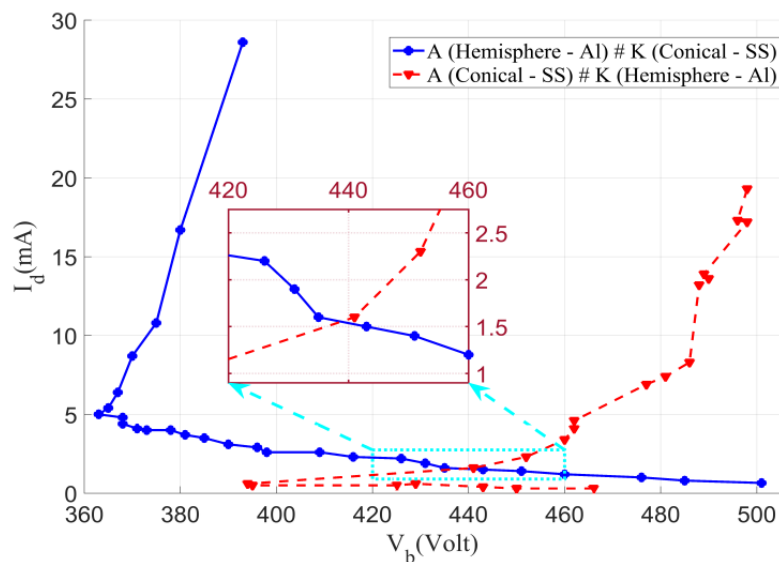


Fig. 8. Breakdown voltage versus electrical discharge current for hemispherical (Al) anode with conical (SS) cathode and compared with the reverse polarity.

3.2 - Hemispherical (Al) and conical (C) electrodes

Figure (9) illustrated the relation between the breakdown voltage and electrical discharge current for:

i- A: Conical (C) - K: Hemispherical (Al)

ii- A: Hemispherical (Al) - K: Conical (C)

The hemispherical (Al) anode with conical (C) cathode gave higher values of electrical discharge current than that of hemispherical (Al) one. This was due to large surface area and high work function material of conical (C) cathode. Moreover, the hemispherical (Al) cathode had the lower $(V_b)_{min}$ value than conical (C) one. Because the low work function of cathode material, Al, which lead to greater ionization efficiency.

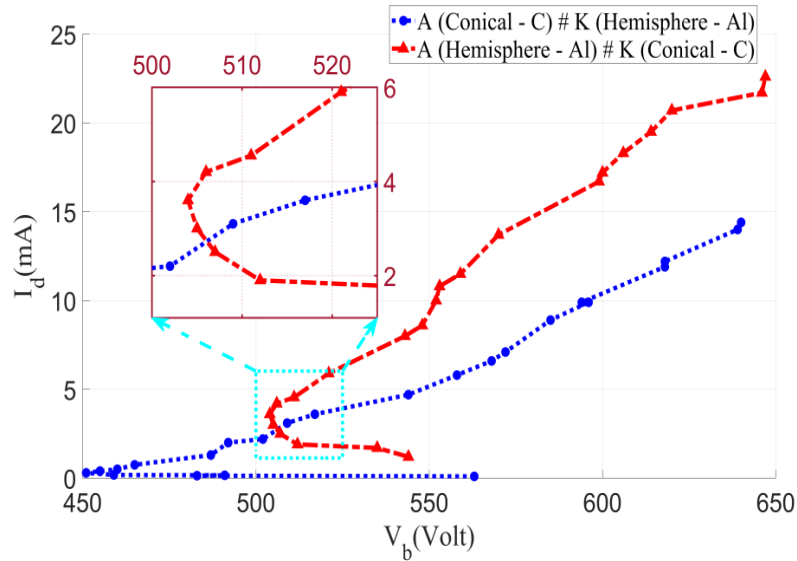


Fig. 9. Breakdown voltage versus electrical discharge current for hemispherical (Al) anode with conical (C) cathode and compared with the reverse polarity.

3.3- Hemispherical (Al) and conical (Al) electrodes

Figure 10 illustrated the relation between the breakdown voltage and electrical discharge current for:

i- A: Hemispherical (Al) - K: Conical (Al)

ii- A: Conical (Al) - K: Hemispherical (Al)

The hemispherical (Al) anode with conical (Al) cathode gave the high values of electrical discharge current. Moreover, the hemispherical (Al) cathode had lower $(V_b)_{\min}$ value than the conical (Al) one. The higher electrical discharge current for the conical cathode had a tip and larger surface area (43.88 cm^2) than that of hemispherical cathode.

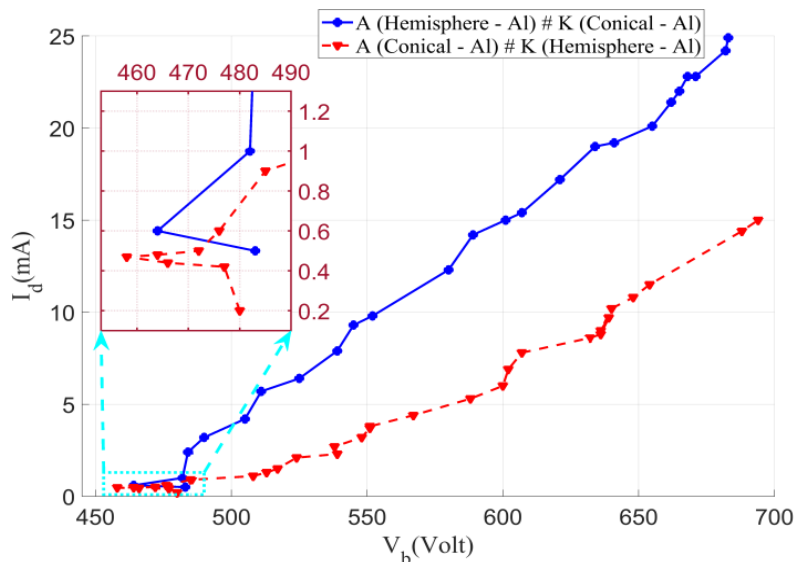


Fig. 10. Breakdown voltage versus electrical discharge current for hemispherical (Al) anode with conical (Al) cathode and compared with the reverse polarity.

3.4- Conical (SS) and spherical (C) electrodes

Figure 11 illustrated the relation between the breakdown voltage and electrical discharge current for:

i- A: Conical (SS) - K: Spherical (C)

ii- A: Spherical (C) - K: Conical (SS)

The spherical (C) anode with conical (SS) cathode gave the high values of discharge current. Because the conical (SS) cathode had lower work function material and higher surface area (conical surface area = 43.88 cm²) than that of spherical (C) cathode. Moreover, the spherical (C) cathode had lower (V_b)_{min.} value than that the conical (SS) one. Because of the surface nature of (C) cathode and the small surface area, sphere shape, which lead to high secondary electron emission and so it needs low voltage to reach the breakdown.

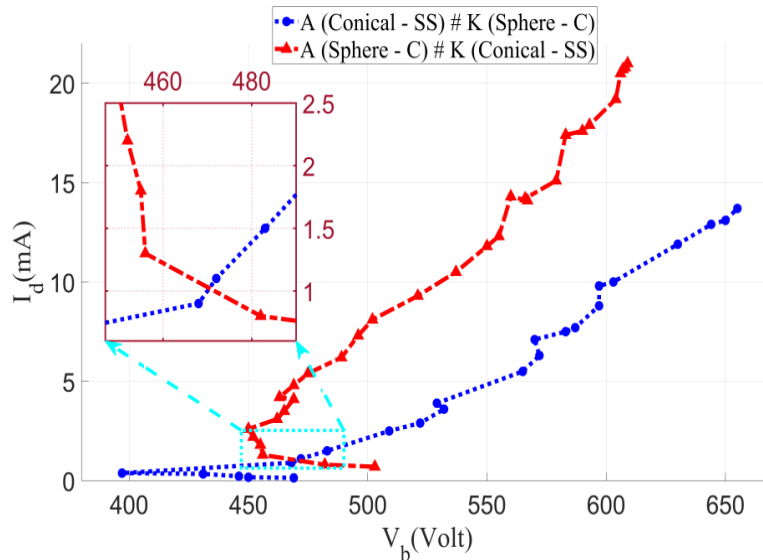


Fig. 11. Breakdown voltage versus electrical discharge current for spherical (C) anode with conical (SS) cathode and compared with the reverse polarity.

3.5- Conical (C) and spherical (C) electrodes

Figure 12 illustrated the relation between the breakdown voltage and electrical discharge current for:

i- A: Conical (C) - K: Spherical (C)

ii- A: Spherical (C) - K: Conical (C)

The spherical (C) anode with conical (C) cathode gave the higher values of electrical discharge current due to large surface area of conical (C) cathode and a tip that concentrated the charges than that of spherical (C) cathode. Moreover, the spherical (C) cathode had lower (V_b)_{min.} value than the conical (C) cathode due to the low surface area of sphere shape.

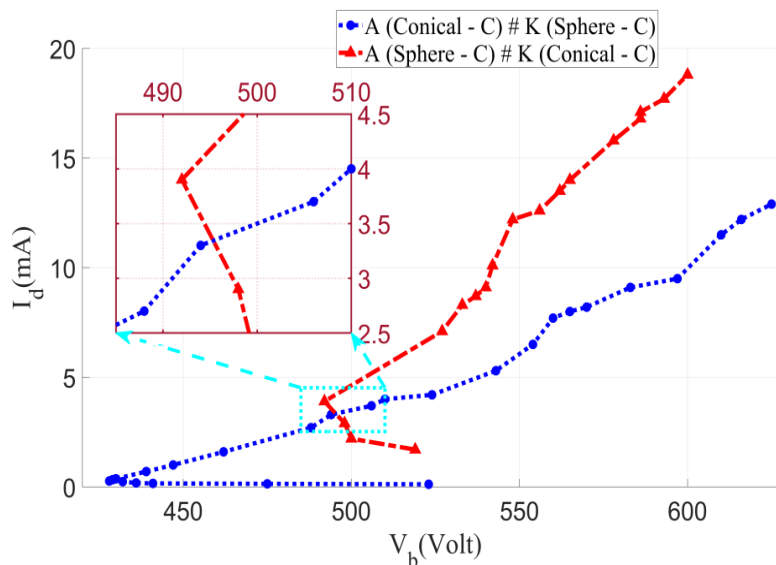


Fig. 12. Breakdown voltage versus electrical discharge current for spherical (C) anode with conical (C) cathode and compared with the reverse polarity.

The hemispherical (Al) anode with conical (SS) cathode had the lowest value of minimum breakdown voltage. The highest value of $(V_b)_{\min.}$ was observed for the hemispherical (Al) anode with conical or hemispherical (C) cathode, presented in Table (2).

TABLE 2. Minimum breakdown voltages values for the different electrical discharge cases at minimum N_2 gas pressure

Case	A	K	V_b (minimum)	Pressure (mTorr)
1	Hemisphere (Al)	Conical (SS)	363 V	680
2	Conical (SS)	Hemisphere (Al)	394 V	264
3	Conical (SS)	Sphere (C)	397 V	297
4	Conical (C)	Sphere (C)	428 V	174
5	Sphere (C)	Conical (SS)	450 V	186
6	Conical (C)	Hemisphere (Al)	451 V	162
7	Conical (Al)	Hemisphere (Al)	458 V	168
8	Hemisphere (Al)	Conical (Al)	464 V	140
9	Hemisphere (C)	Hemisphere (Al)	491 V	153
10	Sphere (C)	Conical (C)	492 V	240
11	Hemisphere (Al)	Hemisphere (Al)	500 V	158
12	Hemisphere (Al)	Conical (C)	504 V	188
13	Hemisphere (Al)	Hemisphere (C)	504 V	153
14	Conical (Al)	Conical (Al)	463 V	208

(B) Paschen Curve

(1) Materials of electrodes

Figures (13-17) show the relation between Pd and V_b for the cases of measured data and fit values with different materials and shapes of electrodes.

1.1- Hemispherical anode and cathode

Figure 13 shows the relation between Pd and breakdown voltage for the following cases:

- i- A: Hemisphere (Al) - K: Hemisphere (Al)
- ii- A: Hemisphere (C) - K: Hemisphere (Al)
- iii- A: Hemisphere (Al) - K: Hemisphere (C)

There was a small difference in the breakdown voltages and their minimal values. A minimum value of Pd, $(Pd)_{\min.}$, would be at the value of $(V_b)_{\min.}$. On the left side of $(Pd)_{\min.}$, the gas pressure was low and the mean free path was large. The probability of ionization collision for electrons with the molecules of N_2 gas was less. It is necessary to have a high voltage that will be needed for the sustainable ionization on each collision. On the right side of $(Pd)_{\min.}$, the gas pressure was high and the mean free path was less. So

the collisions of electrons with the molecules of N_2 gas were very frequent. Moreover, the electrons can't get the required energy which is necessary to ionize the gas molecules. The ionization occurs when a required high voltage gave the electrons a sufficient energy and then breakdown voltage increased as shown in the left side of $(Pd)_{min}$. The corresponding pressure was less due to the same shape of electrodes. Therefore, the number of collisions between an electron and N_2 atom was less and the generation of ions was only a specific number. These ions moved towards the cathode and led to the production of secondary electrons. As a result of the lower number of ions, the rate of secondary electron emission will not frequently change. The breakdown voltages were different for each case at the same Pd value related to the different work functions of materials, Figure (13-d).

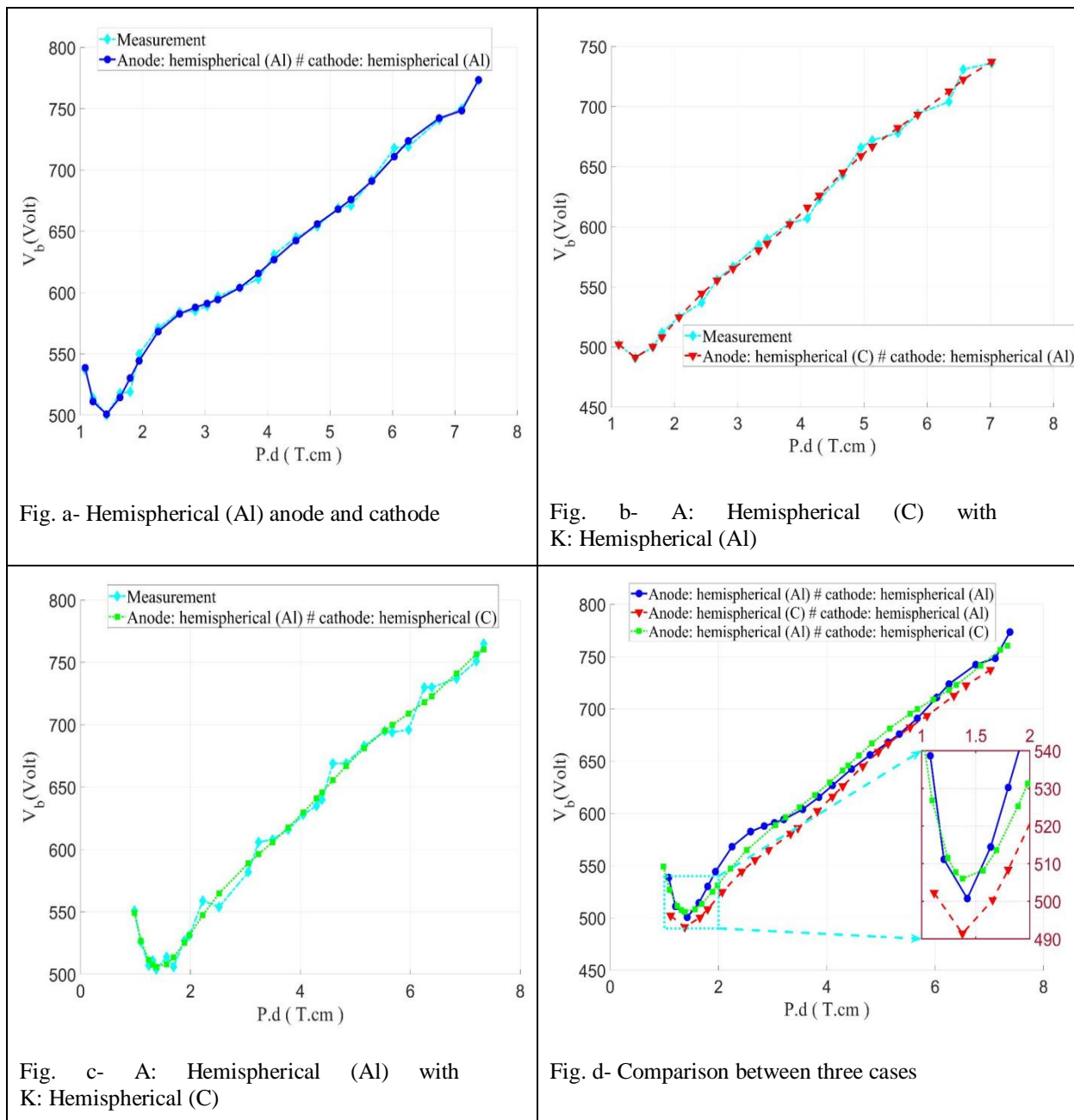


Fig. 13. Paschen curves for hemispherical (Al, C) anodes with hemispherical (C, Al) cathodes and compared with hemispherical (Al) anode and cathode.

(2) Materials and shapes of electrodes

2.1- Hemispherical anode and conical cathode

Figure 14 shows the relation between Pd and breakdown voltage for the following cases:

- i- A: Hemispherical (Al) - K: Conical (SS)
- ii- A: Hemispherical (Al) - K: Conical (C)
- iii- A: Hemispherical (Al) - K: Conical (Al)

Figure (a) illustrated that the Paschen curve was very broad and the minimum value of V_b was at $(Pd)_{min.}$ of 6.12 Torr.cm. Figures (b) and (c) show that the values of $(Pd)_{min.}$ were equal to 1.692 Torr.cm and 1.26 Torr.cm, respectively. There was a small difference in the breakdown voltages for the cathode materials of Al and C, see Figure (d). The (SS) cathode had the lowest value of $(V_b)_{min.}$ because the stainless steel was a hard alloy and the emission of electrons was low.

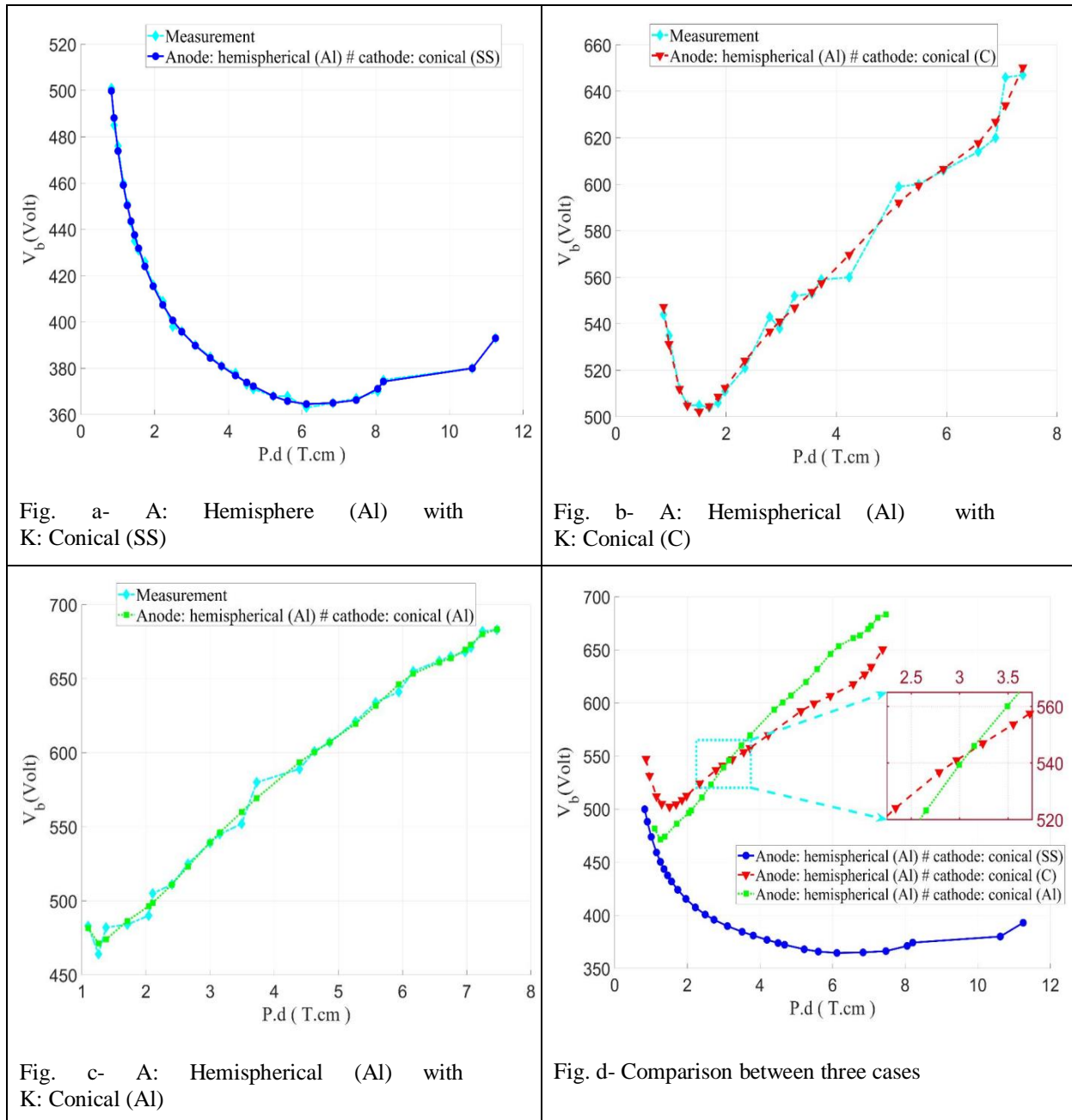


Fig. 14. Paschen curves for hemispherical (Al) anode with conical (Al, C, SS) cathodes.

2.2- Spherical anode and conical cathode

Figure 15 shows the relation between Pd and breakdown voltage for the following cases:

i- A: Spherical (C) - K: Conical (SS)

ii- A: Spherical (C) - K: Conical (C)

The values of breakdown voltages for the conical (C) cathode was higher than that of conical (SS) one. The minimum value of Pd for conical (SS) cathode was lower than that for conical (C) one. This is due to that the secondary electron emission of conical (C) cathode is lower than that of conical (SS) cathode.

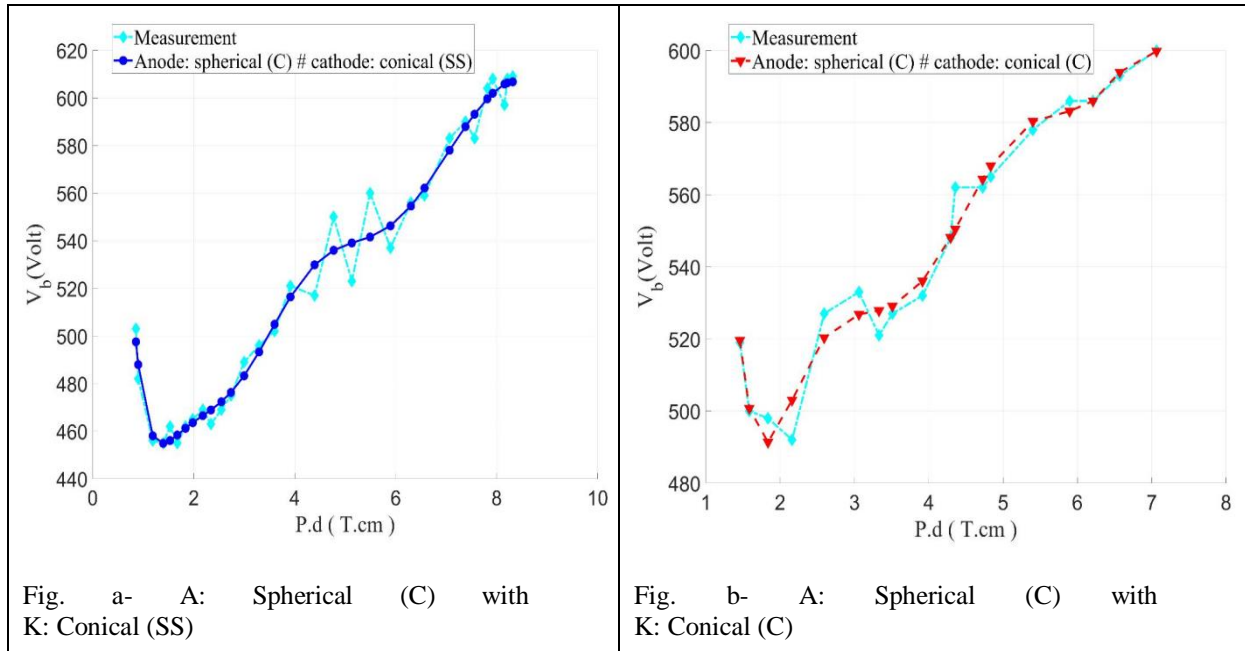


Fig. a- A: Spherical (C) with K: Conical (SS)

Fig. b- A: Spherical (C) with K: Conical (C)

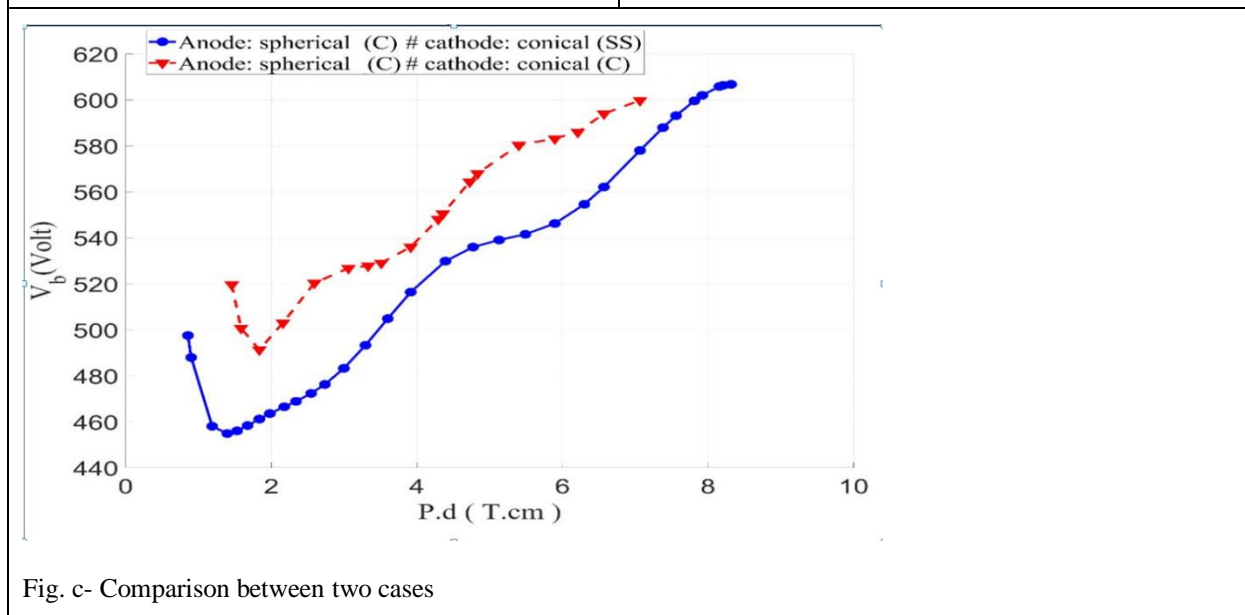


Fig. c- Comparison between two cases

Fig. 15. Paschen curves for spherical (C) anode with conical (C, SS) cathodes cases.

2.3- Conical anode and spherical cathode

Figure (16) shows the relation between Pd and breakdown voltage for the following cases:

i- A: Conical (C) - K: Spherical (C)

ii- A: Conical (SS) - K: Spherical (C)

The value of $(V_b)_{min}$. for the conical (SS) anode was lower than that of conical (C) one. On the left side of $(Pd)_{min}$., there was a small variation in the breakdown voltages. This indicated that the difference in material of anode doesn't have a noticeable effect on the values of breakdown voltages. The value of

$(Pd)_{min.}$ for conical (C) anode was equal to 1.566 Torr.cm and lower than that for conical (SS) anode (2.673 Torr.cm).

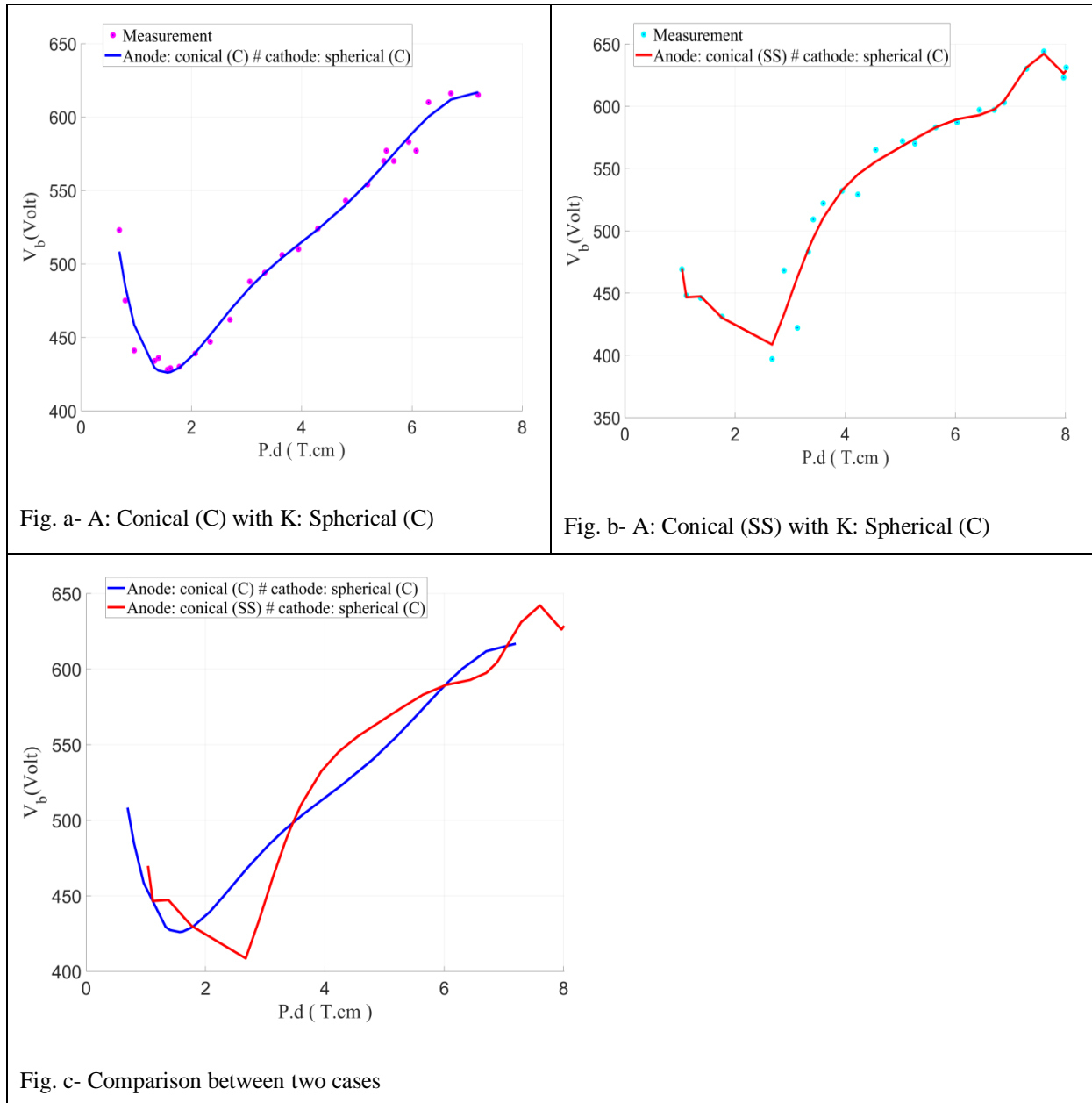


Fig. 16. Paschen curves for conical (C, SS) anodes with spherical (C) cathode.

2.4- Conical anode and hemisphere cathode

Figure (17) shows the relation between Pd and breakdown voltage for the following cases:

- i- A: Conical (Al) - K: Hemispherical (Al)
- ii- A: Conical (C) - K: Hemispherical (Al)
- iii- A: Conical (SS) - K: Hemispherical (Al)

A small difference in the values of breakdown voltages for the conical (Al) anode and conical (SS) one was observed. While the conical (C) anode had the lowest values of breakdown voltages. It is clear that the $Pd_{min.}$ of conical (C) anode (2.376 Torr.cm) is higher than that of conical aluminum (1.512 Torr.cm) and conical stainless steel (1.458 Torr.cm) anodes. This is due to the work function of (Al) and (SS) are lower than (C). Therefore, the breakdown voltage for conical (Al) and conical (SS) anodes are nearly close and gave the high values in Paschen curve .

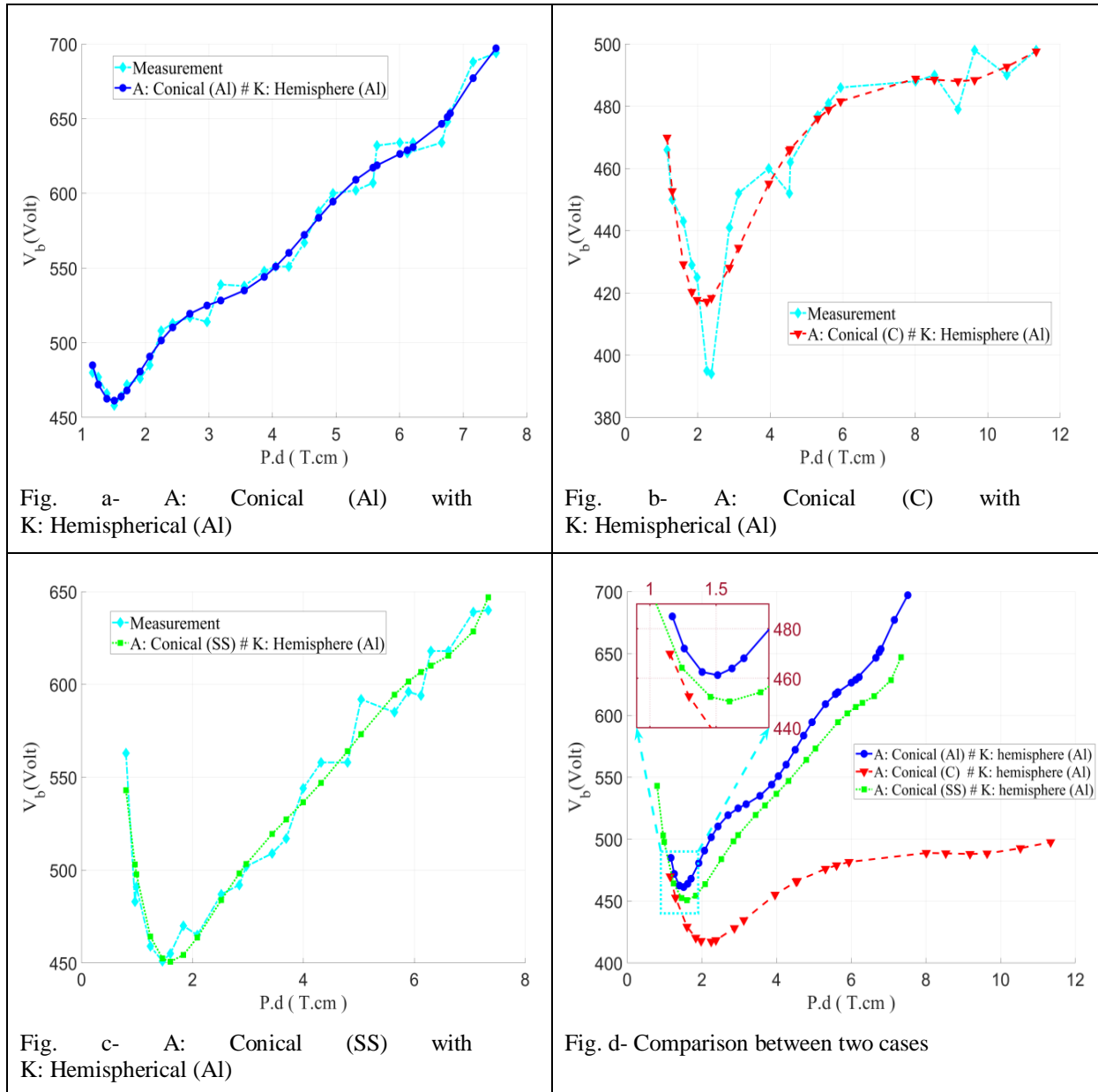


Fig. 17. Paschen curves for conical (Al, SS, C) anodes with hemispherical (Al) cathode.

(C) Modification of Paschen's law

The two important criteria for an electrical breakdown in gases are the availability of primary electrons and the restitution of diffusion loss for electrons and ions [5]. The diffusion loss was compensated by an ionization mechanism which generated the amplification of the ions or electrons. The conventional Paschen's law predicted that the breakdown voltage of a gas depends only on the Pd value [9, 57-59]. There are two factors that play an important role in the discharge characteristics and led to the modification in the conventional Paschen's law. They are the materials and shapes of anode and cathode electrodes. Paschen's law described the characteristics of gas breakdown voltage between the two electrodes. Müller and De La Rue presented that the potential depends on the gas quantity between the parallel electrodes at a constant temperature [60]. Afterward, Paschen extended these observations to be related to the spherical electrodes with variable spacing and measured the breakdown voltage at different gas pressures and inter-electrode distances. A minimum value of potential was necessary to excite the discharge and proportional to the product of gas pressure and gap distance for all pressure values down to a limiting critical value [61]. For any two discharge arrangements of different values of pressure, P_1 and P_2 , and separation distances, d_1 and d_2 , will have the same breakdown voltage, V_{b1} and V_{b2} . This is achieved if:

$$P_1 d_1 = P_2 d_2 \tag{2}$$

The deviations from the conventional Paschen's law occurred if there was a difference in the distribution of electric field. The discharge cases in our study could not obey the equation (2), otherwise they had the same $(V_b)_{min.}$. There was an important role for the work function of materials and surface areas of electrodes (anode and cathode). So that the Paschen's law was modified. In this study, there was an effect of electrodes' shapes and materials on the values of minimal breakdown voltages. From Table (2), we found that each two discharge cases had the same $(V_b)_{min.}$ value. Table (3) is divided into five groups according to the same minimum breakdown voltage to reach the required form which related to the equation (2).

TABLE 3. Groups of different discharge cases with the same minimum V_b value to reach the required form of equation (2).

<p>Group (A)</p> <p>Conical (SS) anodes with spherical and/or hemispherical (C and Al) cathodes</p>		<p>Anodes: conical shapes with the same materials (middle between the work functions of cathodes' materials)</p> <p>Cathodes: hemispherical and/or spherical shapes with the different materials and also different than anodes, where $\phi_{A1} = \phi_{A2}$, $\phi_{K1} > \phi_{A1}$ and $\phi_{A2} > \phi_{K2}$</p>		
Case	A	K	V_b (minimum)	Pressure (mTorr)
3	Conical (SS) $\phi_{A1} = 4.4 \text{ eV}$ $S_{A1} = 43.88 \text{ cm}^2$	Sphere (C) $\phi_{K1} = 5 \text{ eV}$ $S_{K1} = 5 \text{ cm}^2$	397 V	$P_1 = 297$
2	Conical (SS) $\phi_{A2} = 4.4 \text{ eV}$ $S_{A2} = 43.88 \text{ cm}^2$	Hemisphere (Al) $\phi_{K2} = 4.28 \text{ eV}$ $S_{K2} = 5 \text{ cm}^2$	394 V	$P_2 = 264$
$P_1 d_1 = P_2 d_2 * x$ $(297) * (9) = (264) * (9) * x \quad \text{then } x = 1.125$ $x = \frac{S_{A1} + S_{K1}}{S_{A1}} * y$ $1.125 = 1.1139 * y \quad \text{then } y = 1.00996 \approx \frac{\phi_{A2}}{\phi_{K2}}$ <p>So</p> $P_1 d_1 = P_2 d_2 * \left(\frac{S_{A2} + S_{K2}}{S_{A2}} \right) * \frac{\phi_{A2}}{\phi_{K2}}$ <p>Or</p> $P_1 d_1 = P_2 d_2 * \left(\frac{S_{A1} + S_{K1}}{S_{A1}} \right) * \frac{\phi_{A2}}{\phi_{K2}}$			$\frac{\phi_{A2}}{\phi_{K2}} = \frac{4.4}{4.28} = 1.028$ <p>-----</p> $\frac{S_{A1} + S_{K1}}{S_{A1}} = \frac{43.88 + 5}{43.88} = 1.1139$ <p>Also</p> $\frac{S_{A2} + S_{K2}}{S_{A2}} = \frac{5 + 43.88}{43.88} = 1.1139$	
<p>Group (B)</p> <p>Conical and spherical or</p>		<p>Anodes: one anode conical electrode and the other spherical/hemispherical one with the same materials</p>		

	$S_{A1} = 5 \text{ cm}^2$	$S_{K1} = 43.88 \text{ cm}^2$		
9	Hemisphere (C) $\varphi_{A2} = 5 \text{ eV}$ $S_{A2} = 5 \text{ cm}^2$	Hemisphere (Al) $\varphi_{K2} = 4.28 \text{ eV}$ $S_{K2} = 5 \text{ cm}^2$	491 V	$P_2 = 153$
$P_1 d_1 = P_2 d_2 * x$ $(240) * (9) = (153) * (9) * x$ then $x = 1.568$ $x = \frac{S_{A1} + S_{K1}}{S_{K1}} * y$ $1.568 = 2 * y$ then $y = 0.784 \approx \frac{\varphi_{K1}}{\varphi_{K2}} = \frac{\varphi_{K1}}{\varphi_{A1}}$ So $P_1 d_1 = P_2 d_2 * \left(\frac{S_{A2} + S_{K2}}{S_{K2}}\right) * \frac{\varphi_{K1}}{\varphi_{K2}}$ Or $P_1 d_1 = P_2 d_2 * \left(\frac{S_{A2} + S_{K2}}{S_{A2}}\right) * \frac{\varphi_{K1}}{\varphi_{A1}}$ Or $P_1 d_1 = P_2 d_2 * \left(\frac{S_{A2} + S_{K2}}{S_{A2}}\right) * \frac{\varphi_{K1}}{\varphi_{K2}}$ Or $P_1 d_1 = P_2 d_2 * \left(\frac{S_{A2} + S_{K2}}{S_{K2}}\right) * \frac{\varphi_{K1}}{\varphi_{A1}}$			$\frac{\varphi_{K1}}{\varphi_{A1}} = \frac{4.28}{5} = 0.856$ Or $\frac{\varphi_{K1}}{\varphi_{K2}} = \frac{4.28}{5} = 0.856$ ----- $\frac{S_{A2} + S_{K2}}{S_{K2}} = \frac{5 + 5}{5} = 2$ Or $\frac{S_{A2} + S_{K2}}{S_{A2}} = \frac{5 + 5}{5} = 2$	
Group (D) Spherical and/or hemispherical (Al) anodes <u>with</u> conical and spherical and/or hemispherical (C) cathodes		<u>Anodes:</u> spherical and/or hemispherical shapes with the same materials <u>Cathodes:</u> one cathode spherical and/or hemispherical electrode and the other conical one with the same materials (higher than anode material), where $\varphi_{A1} = \varphi_{A2}$ & $\varphi_{K1} = \varphi_{K2}$ & $\varphi_{K1} > \varphi_{A1}$		
Case	A	K	V_b (minimum)	Pressure (mTorr)
12	Hemisphere (Al) $\varphi_{A1} = 4.28 \text{ eV}$ $S_{A1} = 5 \text{ cm}^2$	Conical (C) $\varphi_{K1} = 5 \text{ eV}$ $S_{K1} = 43.88 \text{ cm}^2$	504 V	$P_1 = 188$

8	Hemisphere (A1) $\phi_{A2} = 4.28 \text{ eV}$ $S_{A2} = 5 \text{ cm}^2$	Conical (A1) $\phi_{K2} = 4.28 \text{ eV}$ $S_{K2} = 43.88 \text{ cm}^2$	464 V	$P_2 = 140$
$P_1 d_1 = P_2 d_2 * x$ $(208) * (9) = (140) * (9) * x$ then $x = 1.485 \approx \sqrt{2}$ $x = \left(\frac{S_{A1} + S_{K1}}{S_{K1}} \right)^{1/2}$ <p style="text-align: center;">So</p> $P_1 d_1 = P_2 d_2 * \left(\frac{S_{A1} + S_{K1}}{S_{K1}} \right)^{1/2} * \left(\frac{\phi_{K1}}{\phi_{A1}} \right)^2$ <p>Or</p> $P_1 d_1 = P_2 d_2 * \left(\frac{S_{A1} + S_{K1}}{S_{K1}} \right)^{1/2} * \left(\frac{\phi_{K2}}{\phi_{A2}} \right)^2$			$\frac{\phi_{K1}}{\phi_{A1}} = \frac{4.28}{4.28} = 1$ <p style="text-align: center;">Or</p> $\frac{\phi_{K1}}{\phi_{K2}} = \frac{4.28}{4.28} = 1$ <p style="text-align: center;">-----</p> $\frac{S_{A1} + S_{K1}}{S_{K1}} = \frac{43.88 + 43.88}{43.88} = 2$	

Then, we can summarize the Table (3) to be in another form which illustrated a general equation for each group, see Table (4).

TABLE 4. General equation for each group consisting of two discharge cases with the same $(V_b)_{min.}$

Group (A)	<p><u>Anodes:</u> same materials and same surface areas</p> <p><u>Cathodes:</u> different materials and same surface areas</p> $P_1 d_1 = P_2 d_2 * \left(\frac{S_{A2} + S_{K2}}{S_{A2}} \right) * \frac{\phi_{A2}}{\phi_{K2}}$ <p>Where $d_1 = d_2 = 9 \text{ cm}, P_1 > P_2$</p> <table border="1" style="width: 100%; border-collapse: collapse;"> <tr> <td style="width: 10%; text-align: center;">P_1</td> <td style="width: 40%;">minimum pressure at $(V_b)_{min.}$ in Paschen curve for 1st discharge case, i.e. (with high $Pd_{min.}$ value)</td> <td style="width: 10%; text-align: center;">P_2</td> <td style="width: 40%;">minimum pressure at $(V_b)_{min.}$ in Paschen curve for 2nd discharge case, i.e. (with low $Pd_{min.}$ value)</td> </tr> <tr> <td style="text-align: center;">S_{A2}</td> <td>Surface area of anode for discharge case with low $Pd_{min.}$</td> <td style="text-align: center;">S_{K2}</td> <td>Surface area of cathode for discharge case with low $Pd_{min.}$</td> </tr> <tr> <td style="text-align: center;">ϕ_{A2}</td> <td>Work function of anode material for discharge case with low $Pd_{min.}$</td> <td style="text-align: center;">ϕ_{K2}</td> <td>Work function of cathode material for discharge case with low $Pd_{min.}$</td> </tr> </table>				P_1	minimum pressure at $(V_b)_{min.}$ in Paschen curve for 1 st discharge case, i.e. (with high $Pd_{min.}$ value)	P_2	minimum pressure at $(V_b)_{min.}$ in Paschen curve for 2 nd discharge case, i.e. (with low $Pd_{min.}$ value)	S_{A2}	Surface area of anode for discharge case with low $Pd_{min.}$	S_{K2}	Surface area of cathode for discharge case with low $Pd_{min.}$	ϕ_{A2}	Work function of anode material for discharge case with low $Pd_{min.}$	ϕ_{K2}	Work function of cathode material for discharge case with low $Pd_{min.}$
P_1	minimum pressure at $(V_b)_{min.}$ in Paschen curve for 1 st discharge case, i.e. (with high $Pd_{min.}$ value)	P_2	minimum pressure at $(V_b)_{min.}$ in Paschen curve for 2 nd discharge case, i.e. (with low $Pd_{min.}$ value)													
S_{A2}	Surface area of anode for discharge case with low $Pd_{min.}$	S_{K2}	Surface area of cathode for discharge case with low $Pd_{min.}$													
ϕ_{A2}	Work function of anode material for discharge case with low $Pd_{min.}$	ϕ_{K2}	Work function of cathode material for discharge case with low $Pd_{min.}$													
Group (B)	<p><u>Anodes:</u> same materials and different surface areas</p> <p><u>Cathodes:</u> different materials and different surface areas</p>															

	$P_1 d_1 = P_2 d_2 * \left(\frac{S_{A2} + S_{K2}}{S_{A2}} \right) * \frac{\varphi_{K1}}{\varphi_{K2}}$ <p>Where $d_1 = d_2 = 9 \text{ cm}, P_1 > P_2$</p> <table border="1" style="width: 100%; border-collapse: collapse;"> <tr> <td style="width: 10%; text-align: center;">P_1</td> <td style="width: 40%;">minimum pressure at $(V_b)_{\min.}$ in Paschen curve for 1st discharge case, i.e. (with high $Pd_{\min.}$ value)</td> <td style="width: 10%; text-align: center;">P_2</td> <td style="width: 40%;">minimum pressure at $(V_b)_{\min.}$ in Paschen curve for 2nd discharge case, i.e. (with low $Pd_{\min.}$ value)</td> </tr> <tr> <td style="text-align: center;">S_{A2}</td> <td>Surface area of anode for discharge case with low $Pd_{\min.}$</td> <td style="text-align: center;">S_{K2}</td> <td>Surface area of cathode for discharge case with low $Pd_{\min.}$</td> </tr> <tr> <td style="text-align: center;">φ_{K1}</td> <td>Work function of cathode material for discharge case with high $Pd_{\min.}$</td> <td style="text-align: center;">φ_{K2}</td> <td>Work function of cathode material for discharge case with low $Pd_{\min.}$</td> </tr> </table>				P_1	minimum pressure at $(V_b)_{\min.}$ in Paschen curve for 1 st discharge case, i.e. (with high $Pd_{\min.}$ value)	P_2	minimum pressure at $(V_b)_{\min.}$ in Paschen curve for 2 nd discharge case, i.e. (with low $Pd_{\min.}$ value)	S_{A2}	Surface area of anode for discharge case with low $Pd_{\min.}$	S_{K2}	Surface area of cathode for discharge case with low $Pd_{\min.}$	φ_{K1}	Work function of cathode material for discharge case with high $Pd_{\min.}$	φ_{K2}	Work function of cathode material for discharge case with low $Pd_{\min.}$
P_1	minimum pressure at $(V_b)_{\min.}$ in Paschen curve for 1 st discharge case, i.e. (with high $Pd_{\min.}$ value)	P_2	minimum pressure at $(V_b)_{\min.}$ in Paschen curve for 2 nd discharge case, i.e. (with low $Pd_{\min.}$ value)													
S_{A2}	Surface area of anode for discharge case with low $Pd_{\min.}$	S_{K2}	Surface area of cathode for discharge case with low $Pd_{\min.}$													
φ_{K1}	Work function of cathode material for discharge case with high $Pd_{\min.}$	φ_{K2}	Work function of cathode material for discharge case with low $Pd_{\min.}$													
Group (C)	<p><u>Anodes:</u> same materials and same surface areas</p> <p><u>Cathodes:</u> different materials and different surface areas</p> $P_1 d_1 = P_2 d_2 * \left(\frac{S_{A2} + S_{K2}}{S_{A2}} \right) * \frac{\varphi_{K1}}{\varphi_{K2}}$ <p>Where $d_1 = d_2 = 9 \text{ cm}, P_1 > P_2$</p> <table border="1" style="width: 100%; border-collapse: collapse;"> <tr> <td style="width: 10%; text-align: center;">P_1</td> <td style="width: 40%;">minimum pressure at $(V_b)_{\min.}$ in Paschen curve for 1st discharge case, i.e. (with high $Pd_{\min.}$ value)</td> <td style="width: 10%; text-align: center;">P_2</td> <td style="width: 40%;">minimum pressure at $(V_b)_{\min.}$ in Paschen curve for 2nd discharge case, i.e. (with low $Pd_{\min.}$ value)</td> </tr> <tr> <td style="text-align: center;">S_{A2}</td> <td>Surface area of anode for discharge case with low $Pd_{\min.}$</td> <td style="text-align: center;">S_{K2}</td> <td>Surface area of cathode for discharge case with low $Pd_{\min.}$</td> </tr> <tr> <td style="text-align: center;">φ_{K1}</td> <td>Work function of cathode material for discharge case with high $Pd_{\min.}$</td> <td style="text-align: center;">φ_{K2}</td> <td>Work function of cathode material for discharge case with low $Pd_{\min.}$</td> </tr> </table>				P_1	minimum pressure at $(V_b)_{\min.}$ in Paschen curve for 1 st discharge case, i.e. (with high $Pd_{\min.}$ value)	P_2	minimum pressure at $(V_b)_{\min.}$ in Paschen curve for 2 nd discharge case, i.e. (with low $Pd_{\min.}$ value)	S_{A2}	Surface area of anode for discharge case with low $Pd_{\min.}$	S_{K2}	Surface area of cathode for discharge case with low $Pd_{\min.}$	φ_{K1}	Work function of cathode material for discharge case with high $Pd_{\min.}$	φ_{K2}	Work function of cathode material for discharge case with low $Pd_{\min.}$
P_1	minimum pressure at $(V_b)_{\min.}$ in Paschen curve for 1 st discharge case, i.e. (with high $Pd_{\min.}$ value)	P_2	minimum pressure at $(V_b)_{\min.}$ in Paschen curve for 2 nd discharge case, i.e. (with low $Pd_{\min.}$ value)													
S_{A2}	Surface area of anode for discharge case with low $Pd_{\min.}$	S_{K2}	Surface area of cathode for discharge case with low $Pd_{\min.}$													
φ_{K1}	Work function of cathode material for discharge case with high $Pd_{\min.}$	φ_{K2}	Work function of cathode material for discharge case with low $Pd_{\min.}$													
Group (D)	<p><u>Anodes:</u> same materials and same surface areas</p> <p><u>Cathodes:</u> same materials and different surface areas</p> $P_1 d_1 = P_2 d_2 * \left(\frac{S_{K1}}{S_{A1} + S_{K1}} \right) * \left(\frac{\varphi_K}{\varphi_A} \right)^2$ <p>Where $d_1 = d_2 = 9 \text{ cm}, P_1 > P_2$</p> <table border="1" style="width: 100%; border-collapse: collapse;"> <tr> <td style="width: 10%; text-align: center;">P_1</td> <td style="width: 40%;">minimum pressure at $(V_b)_{\min.}$ in Paschen curve for 1st discharge case, i.e. (with high $Pd_{\min.}$ value)</td> <td style="width: 10%; text-align: center;">P_2</td> <td style="width: 40%;">minimum pressure at $(V_b)_{\min.}$ in Paschen curve for 2nd discharge case, i.e. (with low $Pd_{\min.}$ value)</td> </tr> <tr> <td style="text-align: center;">S_{A1}</td> <td>Surface area of anode for discharge case with high $Pd_{\min.}$</td> <td style="text-align: center;">S_{K1}</td> <td>Surface area of cathode for discharge case with high $Pd_{\min.}$</td> </tr> <tr> <td style="text-align: center;">φ_A</td> <td>Work function of anode material for any discharge case</td> <td style="text-align: center;">φ_K</td> <td>Work function of cathode material for any discharge case</td> </tr> </table>				P_1	minimum pressure at $(V_b)_{\min.}$ in Paschen curve for 1 st discharge case, i.e. (with high $Pd_{\min.}$ value)	P_2	minimum pressure at $(V_b)_{\min.}$ in Paschen curve for 2 nd discharge case, i.e. (with low $Pd_{\min.}$ value)	S_{A1}	Surface area of anode for discharge case with high $Pd_{\min.}$	S_{K1}	Surface area of cathode for discharge case with high $Pd_{\min.}$	φ_A	Work function of anode material for any discharge case	φ_K	Work function of cathode material for any discharge case
P_1	minimum pressure at $(V_b)_{\min.}$ in Paschen curve for 1 st discharge case, i.e. (with high $Pd_{\min.}$ value)	P_2	minimum pressure at $(V_b)_{\min.}$ in Paschen curve for 2 nd discharge case, i.e. (with low $Pd_{\min.}$ value)													
S_{A1}	Surface area of anode for discharge case with high $Pd_{\min.}$	S_{K1}	Surface area of cathode for discharge case with high $Pd_{\min.}$													
φ_A	Work function of anode material for any discharge case	φ_K	Work function of cathode material for any discharge case													

Group (E)	<u>Anodes: same materials and different surface areas</u>			
	<u>Cathodes: same materials and same surface areas</u>			
	$P_1 d_1 = P_2 d_2 * \left(\frac{S_{A1} + S_{K1}}{S_{K1}} \right)^{1/2} * \left(\frac{\varphi_K}{\varphi_A} \right)^2$			
	Where $d_1 = d_2 = 9 \text{ cm}$, $P_1 > P_2$			
P_1	minimum pressure at $(V_b)_{\min}$. in Paschen curve for 1 st discharge case, i.e. (with high Pd_{\min} . value)	P_2	minimum pressure at $(V_b)_{\min}$. in Paschen curve for 2 nd discharge case, i.e. (with low Pd_{\min} . value)	
S_{A1}	Surface area of anode for discharge case with high Pd_{\min} .	S_{K1}	Surface area of cathode for discharge case with high Pd_{\min} .	
φ_A	Work function of anode material for any discharge case	φ_K	Work function of cathode material for any discharge case	

From Table (4), we can deduced the modified Paschen's law in a generalized formalism and illustrated in Table (5). This Table is divided into four general equations according to the materials and shapes of cathodes of each group having the same $(V_b)_{\min}$. value.

TABLE 5. Modified Paschen's law in a generalized formalism

(i)	<p><u>Cathodes with different materials and different surface areas</u></p> $P_1 d_1 = P_2 d_2 * \left(\frac{S_{A2} + S_{K2}}{S_{A2}} \right) * \frac{\varphi_{K1}}{\varphi_{K2}}$ <p>Where: Anodes with same materials and same/different surface areas</p>
(ii)	<p><u>Cathodes with different materials and same surface areas</u></p> $P_1 d_1 = P_2 d_2 * \left(\frac{S_{A2} + S_{K2}}{S_{A2}} \right) * \frac{\varphi_{A2}}{\varphi_{K2}}$ <p>Where: Anodes with same materials and same surface areas</p>
(iii)	<p><u>Cathodes with same materials and different surface areas</u></p> $P_1 d_1 = P_2 d_2 * \left(\frac{S_{K1}}{S_{A1} + S_{K1}} \right) * \left(\frac{\varphi_K}{\varphi_A} \right)^2$ <p>Where: Anodes with same materials and same surface areas</p>

(iv)	<p><u>Cathodes with same materials and same surface areas</u></p> $P_1 d_1 = P_2 d_2 * \left(\frac{S_{A1} + S_{K1}}{S_{K1}} \right)^{1/2} * \left(\frac{\varphi_K}{\varphi_A} \right)^2$ <p>Where: Anodes with same materials and different surface areas</p>
<p>Where: The subscript (1) denotes the discharge case of high $(Pd)_{\min}$ value and subscript (2) denotes the discharge case of low $(Pd)_{\min}$ value. The subscripts A and K denote the anode and cathode electrodes, respectively. The S and φ indicate the surface area and work function of electrode's material, respectively.</p>	

Then the breakdown voltage was not only as a function on the product of gas pressure and inter-electrode distance, but also on the ratio of the work function materials and surface areas of electrodes.

Conclusions

In this work, the d.c. glow discharge of hemispherical, spherical, and conical electrodes was investigated using nitrogen gas. The electrodes' materials from aluminum, graphite, and stainless steel were used. From the experimental results, it was concluded that:

- 1- The cathode material of high work function than anode gave the highest discharge current in case of hemispherical electrodes with the same and different materials.
- 2- From a comparison between the same and different electrodes' materials, the highest discharge current was for the conical stainless steel cathode in the case of:
 - Hemispherical anode with conical cathode
 - Spherical anode with conical cathode
 - Conical anode with spherical cathode
- 3- For the conical anode of the same and different materials of hemispherical cathode, the highest discharge current was for the conical graphite anode.
- 4- In case of the electrodes' polarity, it was concluded that the highest electrical discharge current was for:
 - Conical (SS) cathode (in case of A: hemispherical Al and K: conical SS)
 - Conical (C) cathode (in case of A: hemispherical Al and K: conical C)
 - Conical (Al) cathode (in case of A: hemispherical Al and K: conical Al)
 - Conical (SS) cathode (in case of A: spherical C and K: conical SS)
 - Conical (C) cathode (in case of A: spherical C and K: conical C)
- 5- In a comparison between the different materials of conical cathodes in case of hemispherical aluminum anode and spherical graphite one, the stainless steel conical cathode had the lowest values of Paschen curve. Moreover, the graphite conical anode had the lowest values in Paschen curve for the case of aluminum hemispherical cathodes.

Finally, it was concluded that the work function of anode and cathode materials with different shapes play an important role in the electrical discharge characteristics. Also, the traditional Paschen's law was modified as a function in the work function of materials and surface areas of electrodes in addition to the product of gas pressure by inter-electrode distance. The general formalism of modified Paschen's law was deduced according to the materials and shapes of cathodes for each group having the same $(V_b)_{\min}$ value of discharge cases.

References

- [1] Langmuir, I., *PNAS USA*, **14**, 627 (1928).
- [2] Marcus, R. K., and Broekaert, J. A. C., “Glow Discharge Plasma in analytical spectrometry”, 1st ed., John Wiley & Sons Ltd., Chichester (2003).
- [3] Gurnett, D. A., Bhattacharjee, A., “Introduction to plasma physics: with space and laboratory applications”, 2nd ed., Cambridge University Press, Cambridge (2017).
- [4] Garamoon, A. A., Samir, A., Elakshar, F. F., Nosair, A., and Kotp, E.F., *IEEE Trans. Plasma Sci.*, **35**, 1 (2007).
- [5] Mathew, P., George, J., Mathews, T. S., and Kurian, P. J., *AIP Advances*, **9**, 025215 (2019).
- [6] La Rue, W. D., and Müller, H. W., *Philos. Trans. R. Soc. London, Ser.*, **171**, 65 (1880).
- [7] Paschen, F., *Ann. Phys.*, 273, 69 (1889).
- [8] Radjenovic, M. R., Radjenovic, B., Klas, M., Bojarov, A., and Matejcik, S., *Acta Phys. Slovaca*, **63**, 105 (2013).
- [9] Peschot, A., Bonifaci, N., Lesaint, O., Valadares, C., and Poulain, C., *Appl. Phys. Lett.*, **105**, 123109 (2014).
- [10] Torres, C., Reyes, P. G., Castillo, F., and Martinez, H., *J. Phys. Conf. Ser.*, **370**, 012067 (2012).
- [11] Meek, J. M., and Craggs, J. D., “Electrical breakdown of gases”, 1st ed., The Clarendon Press Oxford University Press, Oxford and London (1953).
- [12] Reizer, Y., “Gas discharge Physics”, 1st ed., Springer-Verlag, Berlin Heidelberg (1991).
- [13] Boyle, W. S., and Kisliuk, P., *Phys. Review*, **97**, 255 (1955).
- [14] Boyle, W. S., Kisliuk, P., and Germer, L. H., *J. Appl. Phys.*, **26**, 720, 1955.
- [15] Sarkar, J., “Sputtering Materials for VLSI and Thin Film Devices”, 1st ed., Elsevier, Oxford (2014).
- [16] Sahu, B. B., Wen, L., Han, J.G., *Phys. Rev. Appl.*, **10**, 054042 (2018).
- [17] Choi, M. S., Jeon, E. B., Kim, J. Y., Choi, E. H., Lim, J. S., Choi, J., and Park, S. Y., *LWT*, **154**, 112698 (2022).
- [18] Mravlje, J., Regvar, M., and Mikuš, K. V., *J. Fungi (Basel)*, **7**, 650 (2021).
- [19] Noori, H., Khodabakhshi, E., and Jōgi, I., *Nucl. Instrum. Methods Phys. Res. A: Accel. Spectrom. Detect. Assoc. Equip.*, **962**, 163667 (2020).
- [20] Ivankov, A., Capela, T., Rueda, V., Bru, E., Piquet, H., Schitz, D., Florez, D., and Diez, R., *Plasma*, **5**, 75 (2022).
- [21] Chodiseti, S. P., Malik, V. K., and Kumar, B. V. M., *Int. J. Appl. Ceram. Technol.*, **19**, 1367 (2022).
- [22] Vasiliev, M. N., Vasilieva, T. M., and Hein, A. M., *J. Phys. D: Appl. Phys.*, **52**, 335202 (2019).
- [23] Clapa, M., and Gaj, J., *Sens. Actuators, A*, **332**, 113069 (2021).
- [24] Chiad, B. T., Zubaydi, T. L. A., Khalaf, M. K., and Khudiar, A. I., *Indian J. Pure Ap. Phy.*, **48**, 723 (2010).
- [25] Bogaerts, A., Neyts, E., Gijbels, R., and Mullen, J. D., *Spectrochim. Acta, Part B*, **57**, 609 (2002).
- [26] Merche, D., Vandencastelee, N., and Reniers, F., *Thin Solid Films*, **520**, 4219 (2012).
- [27] Wulf, G., Mayer, B., and Lommatzsch, U., *Plasma*, **5**, 44 (2022).

-
- [28] Seo, H. J., Gil, Y. E., Hwang, K. H., and Ananth, A., Boo, J. H., *Electron. Mater. Lett.*, **15**, 396 (2019).
- [29] Bhatt, S., Pulpytel, J., and Aref-Khonsari, F., *Surf. Innovations*, **3**, 63 (2015).
- [30] Zheng, W., Huang, X., and Zheng, J., *Fusion Eng. Des.*, **140**, 23 (2019).
- [31] Alimpijević, M., Rajović, Z., Brajović, D., Vujisić, M., and Stanković, K., *Vacuum*, **99**, 89 (2014).
- [32] Xingnan, L., Zhengang, S., Guojun, Y., and Xunshi, Y., *Ann. Nucl. Energy*, **110**, 1224 (2017).
- [33] Klas, M., Radjenović, M. R., Radjenović, B., Stano, M., and Matejčik, Š., *Nucl. Instrum. Methods Phys. Res. B*, **279**, 96 (2012).
- [34] Živanović, E. N., *Vacuum*, **107**, 62 (2014).
- [35] Noori, H., and Jögi, I., *Phys. Lett. A*, **438**, 128111 (2022).
- [36] El-Zein, A., Talaat, M., and Samir, A., *Vacuum*, **194**, 110614 (2021).
- [37] Lisovskiy, V. A., Osmayev, R. O., Gapon, A. V., Dudin, S. V., Lesnik, I. S., and Yegorenkov, V. D., *Vacuum*, **145**, 19 (2017).
- [38] Fu, Y., Yang, S., Zou, X., Luo, H., and Wang, X., *Phys. Plasmas*, **24**, 023508 (2017).
- [39] Fu, Y., Yang, S., Zou, X., Luo, H., and Wang, X., *Phys. Plasmas*, **23**, 093509 (2016).
- [40] Lisovskii, V. A., and Yakovin, S. D., *Tech. Phys.*, **45**, 727 (2000).
- [41] Lisovskiy, V. A., Yakovin, S. D., and Yegorenkov, V. D., *J. Phys. D Appl. Phys.*, **33**, 2722 (2000).
- [42] Lisovskiy, V. A., Koval, V. A., Yegorenkov, V. D., *Phys. Lett. A*, **375**, 1986 (2011).
- [43] Fu, Y., Parsey, G. M., Verboncoeur, J. P., and Christlieb, A. J., *Phys. Plasmas*, **24**, 113518 (2017).
- [44] Takaki, K., Shimizu, M., Mukaigawa, S., and Fujiwara, T., *IEEE Trans. Plasma Sci.*, **32**, 1 (2004).
- [45] Eliasson, B., and Kogelschatz, U., *IEEE Trans. Plasma Sci.*, **19**, 1063 (1991).
- [46] Carey, W. J., Wiebe, A. J., Nord, R. D., Altgilbers, L. L., *IEEE Pulsed Power Conf.*, **741** (2011).
- [47] Li, L., Zhao, Z., Liu, Y., Li, C., Ren, J., and Li, J., *IEEE Trans. Plasma Sci.*, **47**, 4237 (2019).
- [48] Schoenbach, K. H., and Becker, K., *Eur. Phys. J. D*, **70**, 29 (2016).
- [49] Loveless, A. M., Meng, G., Ying, Q., Wu, F., Wang, K., Cheng, Y., and Garner, A. L., *Sci. Rep.*, **9**, 5669 (2019).
- [50] Braithwaite, N. St. J., *Plasma Sources Sci. Technol.*, **9**, 517 (2000).
- [51] Hassouba, M. A., Elakshar, F. F., and Garamoon, A. A., *Fiz. A*, **112**, 81 (2002).
- [52] Kim, J. Y., Kaganovich, I., and Lee, H. -C., *Plasma Sources Sci. Technol.*, **31**, 033001(2022).
- [53] Viegas, P., Slikboer, E., Bonaventura, Z., Guaitella, O., Sobota, A. and Bourdon, A., *Plasma Sources Sci. Technol.*, **31** 053001(2022).
- [54] Schönherr, T., Nawaz, A., Herdrich, G., Röser, H. -P., and Kurtz, M. A., *J. Propul. Power*, **25**, 380 (2009).
- [55] Al-Khashab, M. A. and Al-Abdullah, A. E., *Raf. J. Sci.*, **23**, 138 (2012).
- [56] Deore, A. V., Patil, B. J., Bhoraskar, V. N., and Dhole, S. D., *Indian J. Pure Appl. Phys.*, **50**, 482 (2012).
- [57] Husain, E., and Nema, R. S., *IEEE Trans. Electr. Insul.*, EI-17, 4 (1982).

-
- [58] Go, D. B., and Pohlman, D. A., *J. Appl. Phys.*, **107**, 103303 (2010).
- [59] Loeb, L. B., and Meek, J. M., “Mechanism of Electric Spark”, 1st ed., Stanford University Press, Stanford (1941).
- [60] La Rue, W. D., and Müller, Philos. Trans. R. Soc. London, **171**, 65 (1880).
- [61] Townsend, J. S., “The theory of Ionization of gases by collision”, 1st ed., Constable and Co., London (1910).